Elevated shear zone loading rate during an earthquake cluster in eastern California

Michael Oskin*
Department of Geological Sciences, University of North Carolina at Chapel Hill, Chapel Hill, North Carolina 27599, USA
Lesley Perg
Department of Geology and Geophysics, University of Minnesota, Minneapolis, Minnesota 55455, USA
Eitan Shelef
Michael Strane
Emily Gurney
Department of Geological Sciences, University of North Carolina at Chapel Hill, Chapel Hill, North Carolina 27599, USA
Brad Singer
Xifan Zhang
Department of Geology and Geophysics, University of Wisconsin, Madison, Wisconsin 53706, USA

ABSTRACT

We compare geodetic velocity to geologic fault slip rates to show that tectonic loading was doubled across the eastern California shear zone (ECSZ) during a cluster of major earthquake activity. New slip rates are presented for six dextral faults that compose the ECSZ in the central Mojave Desert. These rates were determined from displaced alluvial fans dated with cosmogenic ^{10}Be and from a displaced lava flow dated with ^{40}Ar/^{39}Ar. We find that the sum geologic Mojave ECSZ slip rate, ≤6.2 ± 1.9 mm/yr, is only half the present-day geodetically measured velocity of 12 ± 2 mm/yr. These rates account for cumulative fault slip and geodetic observations that span the 60-km-wide shear zone; therefore this difference cannot be attributed to postseismic relaxation. Redistribution of tectonic loading over the earthquake cycle at a regional scale suggests that earthquake clustering may be enhanced via feedback with weakening of ductile shear zones.

Keywords: transient deformation, earthquake clustering, Eastern California shear zone, slip rate, cosmogenic dating.

INTRODUCTION

Major earthquakes may cluster regionally over periods from years to centuries, as observed historically (Kagan and Jackson, 1991) and in paleoseismic records (Marco et al., 1996; Rockwell et al., 2000; Dawson et al., 2003; Dolan et al., 2007). Understanding the origin of this clustering behavior would significantly improve forecasts of near-term seismic hazard. One explanation for short-term clustering is fault loading from postseismic static stress increase and viscoelastic relaxation (Dieterich, 1994; Pollitz et al., 2003). However, this loading is limited in extent and magnitude; thus triggered earthquakes are expected only for faults already close to failure. Because most of the stress on faults that is eventually released as earthquakes arises directly from relative plate motion, changes in how this tectonic loading is partitioned among a set of faults could also give rise to clusters of earthquake activity. Identifying such systematic variation of velocity and its relationship to earthquake clusters has been difficult due to a lack of sufficient geologic and geodetic data across an entire fault system.

As a test for elevated loading rate during an active earthquake cluster, we compare new geologic slip rates against geodetic velocity across six dextral faults that compose the eastern California shear zone (ECSZ) at 34.7°N, in the central Mojave Desert (Fig. 1). Paleoseismic investigations by Rockwell et al. (2000) indicate clusters of earthquake activity on this fault system ca. 9 ka, 4–5 ka, and since 1.5 ka. The most recent cluster also includes historic large earthquakes on two of the six faults—the Camp Rock and Pisgah-Bullion faults ruptured in M_W>7.0 earthquakes in 1992 and 1999, respectively. The geodetic rate of strain accumulation across the Mojave ECSZ was 12 ± 2 mm/yr prior to the M_W 7.3 1992 Landers earthquake (Sauber et al., 1994). Though postseismic relaxation contaminates later geodetic data from the Mojave Desert, elsewhere in the ECSZ, rates since 1992 are consistent with 12 ± 2 mm/yr of strain accumulation (Bennett et al., 2003; Meade and Hager, 2005).

By compiling a complete slip-rate budget we need only compare this to the cumulative geodetic displacement rate across the ECSZ to test for elevated tectonic loading rate. This approach avoids the ambiguity inherent in interpreting overlapping strain fields from closely spaced faults (e.g., Dixon et al., 2003). Another advantage of this approach is that geodetic observations at shear-zone scale are not as sensitive to perturbations to the strain field induced by postseismic afterslip and viscoelastic relaxation. For example, <1 cm of motion due to viscoelastic relaxation was observed >100 km from the 1999 Hector Mine earthquake (Freed et al., 2007).

QUATERNARY FAULT SLIP RATES

Active dextral faults of the central Mojave Desert (Fig. 1) are well suited for compilation of a displacement rate budget across the ECSZ. Major faults here are well documented from near-continuous bedrock exposures (Dibblee, 1961). Paleomagnetism of a widespread tuff marker indicates negligible distributed shear displacement via block rotation (Wells and Hillhouse, 1989). Slip rates that average over more than five earthquakes have thus far been documented for only two of the six dextral faults. One, the Pisgah-Bullion fault, slips at a rate of ~0.8 mm/yr, determined from offset mid- to late Pleistocene basalt flows (Hart et al., 1988). We revise this rate upward to 1.0 ± 0.2 mm/yr based on new mapping and ^{40}Ar/^{39}Ar dating one of

*E-mail: oskin@email.unc.edu.

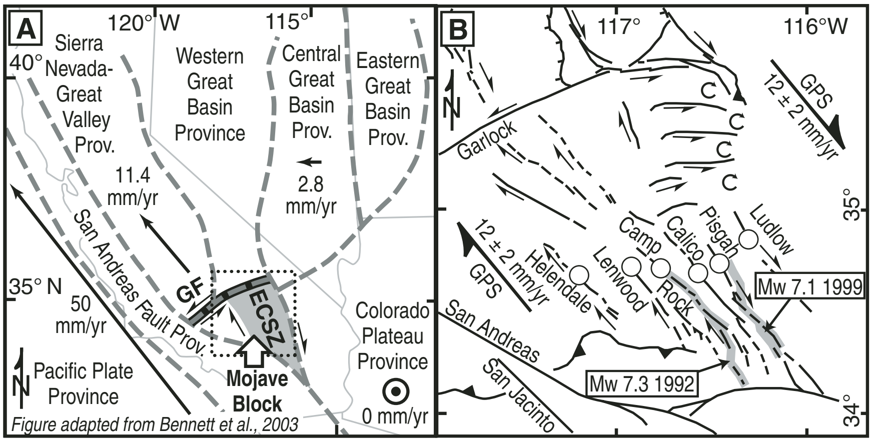

Figure 1. A: Index map of southwest North America showing geodetic provinces from Bennett et al. (2003) and location of Mojave block. Velocities of geodetically stable regions are shown relative to Colorado Plateau. ECSZ—eastern California shear zone in Mojave block. Shear zone continues northward into western Great Basin province. GF—Garlock fault. B: Index map of the Mojave block with active faults and locations of recent earthquake ruptures. Circles show localities of slip-rate measurements that sum to ≤6.2 ± 1.9 mm/yr across the ECSZ. GPS—global positioning system.

these markers (see the GSA Data Repository[1]). The second, the Calico fault, slips at a rate of 1.8 ± 0.3 mm/yr, determined from offset late Pleistocene alluvial fans (Oskin et al., 2007).

In order to complete the slip-rate data set we established new offset measurements and geochronology from late Pleistocene alluvial fans displaced by the Helendale, Lenwood, Camp Rock, and Ludlow faults (Fig. 2). Regionally correlative alluvial fan surfaces, produced by episodic, climate-driven fan aggradation and incision, are present throughout the Mojave Desert region (Bull, 1991). We mapped displaced alluvial fans and inset channels along a portion of each fault with the aid of high-resolution airborne laser scanner topography surveys with resolution of ~2 measurements/m^2 and elevation precision of 10 cm. Fan generations were correlated in the field based on preservation of depositional morphology, inset relationships, and clast weathering, as well as desert varnish, pavement, and soil development (Oskin et al., 2007). Ages of alluvial fan surfaces were determined from in situ accumulation of cosmogenic ^{10}Be in quartz-bearing sediment. We used a high-latitude sea-level ^{10}Be production rate of 5.1 ± 0.3 atoms/g/yr scaled for sample elevation and latitude (Stone, 2000). All ages and slip rates are stated with 95% confidence intervals.

Slip rates of the Lenwood and Helendale faults (Table 1) were defined from displaced $Q2_b$ alluvial fan deposits characterized by subdued depositional morphology, poor to moderately developed pavement, light brown varnish coatings, and poorly to moderately developed argillic soils. Displaced fans dated with the depth-profile method (Anderson et al., 1996) yielded ages of 56 ± 21 ka and 37 ± 7 ka with 50%–70% of the ^{10}Be concentration inherited prior to deposition (Fig. 3). These dates are consistent with a 57 ± 9 ka morphologically similar alluvial fan surface displaced by the Calico fault, where the inherited ^{10}Be concentration was minimal (Oskin et al., 2007).

The Camp Rock and Ludlow faults (Table 1) displace $Q2_a$ alluvial fans and stream terraces characterized by smooth, darkly varnished desert-pavement surfaces and well-developed argillic soils. Amalgamated samples of vein quartz pebbles from preserved fan surfaces southwest of the Camp Rock fault yielded ages of 109 ± 30 ka and 78 ± 28 ka, after subtracting an inherited ^{10}Be concentration estimated from a sample from the sediment source stream. A sample from a portion of the $Q2_a$ fan northeast of the fault yielded an anomalously young 24 ± 28 ka inheritance-corrected age that indicates erosional removal of the original fan depositional surface. All together, these dates are insufficient to confidently assign an age for $Q2_a$. Because $Q2_a$ predates emplacement of $Q2_b$, we use a minimum age of 50 ± 20 ka to conservatively estimate maximum slip rates.

DISCUSSION

Our results (Table 1) show that the pre-1992 12 ± 2 mm/yr geodetic velocity exceeds by a factor of two the ≤6.2 ± 1.9 mm/yr integrated geologic slip rate across the Mojave ECSZ. The discrepancy between geologic and geodetic velocities is unlikely to be the result of significant unrecognized faulting. Active faults with slip rates as low as ~0.4 mm/yr and >5 k.y. span between earthquakes (Rockwell et al., 2000) are well expressed geologically (Dibblee, 1961) and geomorphically in the arid landscape (Fig. 2). We have observed distributed shear in zones to ~2 km wide surrounding ECSZ faults. As described for the case of the Calico fault (Oskin et al., 2007), such deformation accounts for only 10%–30% of fault slip and is overall unlikely to account for the rate discrepancy. Rare ruptures of secondary fault strands with very low (<0.1 mm/yr) rates of activity, such as occurred on the Lavic Lake fault during the 1999 Hector Mine earthquake (Rymer et al., 2002), could account for some additional missing slip. However, accounting for 5 mm/yr of slip over a span of at least 30 k.y. since formation of abundant $Q2_b$ alluvial fan surfaces would require ≥150 m of additional fault displacement. This missing displacement should have produced numerous secondary fault ruptures that would be recognizable in the landscape. The majority of long-term geologic deformation (Dibblee, 1961) and historic earthquake activity has been localized onto known active faults (Fig. 1) where these alluvial fans are demonstrably cut by late Quaternary faulting (Fig. 2).

Elastic strain accumulation from the Mojave section of the San Andreas fault could significantly affect geodetically measured deformation of the ECSZ. The model of Savage and Lisowski (1998), using a locking depth of 25 km, explains as much as 4 mm/yr of excess velocity in the western Mojave Desert. However, such an explanation cannot account for the similarly high geodetic velocity across the ECSZ east of the Sierra Nevada–Great Valley block, farther from the San Andreas fault (Fig. 1). Thus Meade and Hager (2005) found that a self-consistent block-model–based inversion of the geodetic data requires an ~15 km San Andreas fault locking depth and that strain accumulation within the Mojave Desert region is largely attributed to local dextral faulting.

Elevated strain accumulation during an earthquake cluster in the ECSZ supports that time-dependent ductile shear zone strength may modulate tectonic loading and earthquake production on this fault system. Explanation of time-dependent shear zone strength requires both weakening and strengthening over a significant volume of lithosphere at time scales comparable to the earthquake cycle. Dolan et al. (2007) suggested that shear zones undergo strain hardening during periods of elevated loading and anneal and weaken during less active phases. Strain hardening in the ductile regime is most likely to be significant immediately following an earthquake, when high stresses at the base of a rupture can induce transient deformation via glide-controlled creep (Trepmann and Stöckhert,

[1]GSA Data Repository item 2008119, supplemental maps of fault offsets, field photographs, and ^{10}Be and ^{40}Ar/^{39}Ar age data, is available online at www.geosociety.org/pubs/ft2008.htm, or on request from editing@geosociety.org or Documents Secretary, GSA, P.O. Box 9140, Boulder, CO 80301, USA.

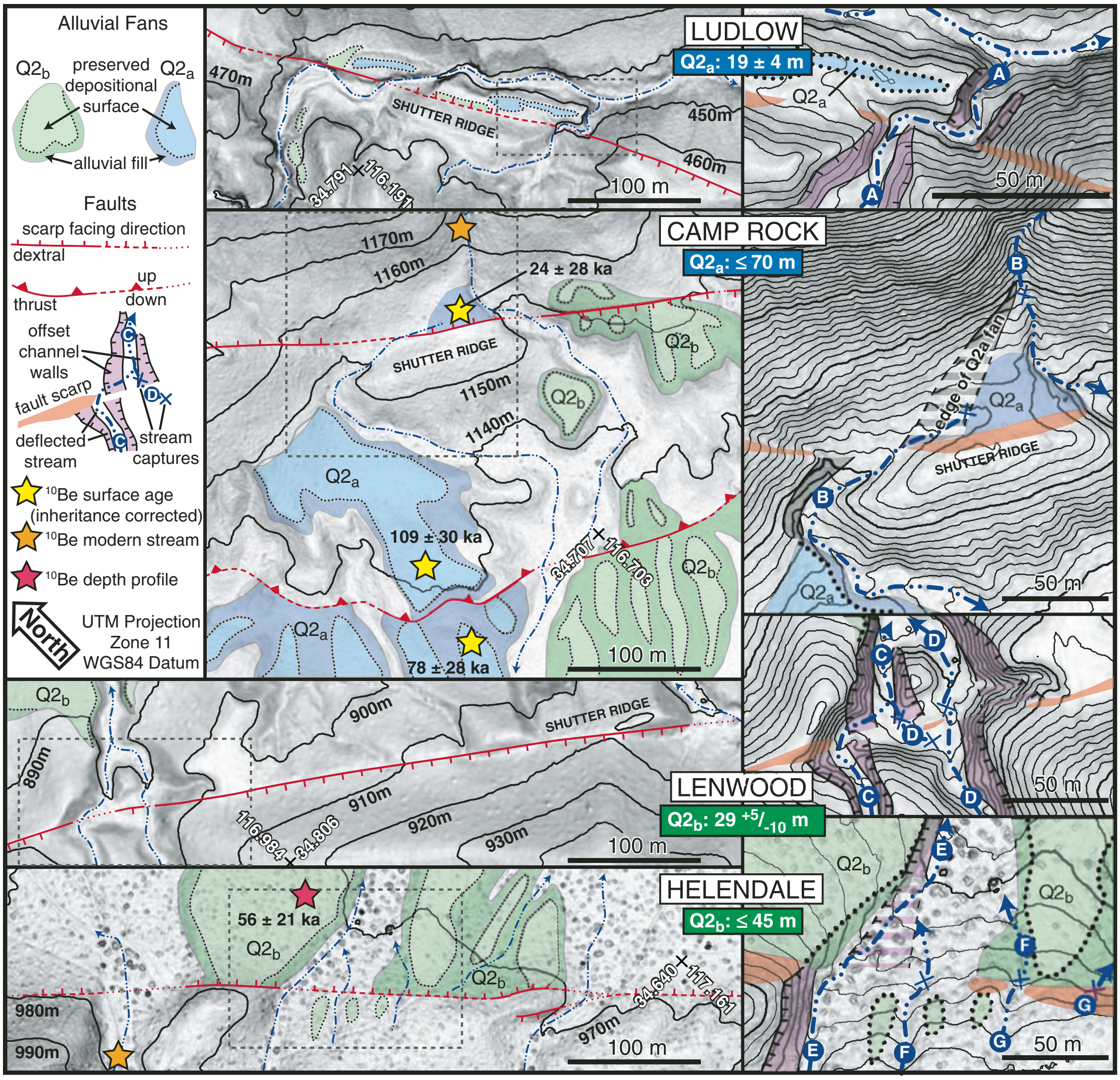

Figure 2. Maps of landforms offset by dextral faults in the Mojave eastern California shear zone. Gray-scale base maps depict topographic slope, with steeper areas darker, overlain by elevation contours: 10 m interval for overview maps, left, and 1 m interval for detail maps, right. Dashed boxes show locations of detail maps. All maps are oriented northwest-southeast, parallel to regional fault strike. Offsets are calculated from displaced inset channel walls except for Camp Rock fault, where up to 70 m offset of a $Q2_a$ alluvial fan edge was measured. Projection of shutter ridges into channels and deflection of streams are consistent with preferred offsets of 19 m and 29 m for the Ludlow and Lenwood faults, respectively. Deflection of stream E and capture of streams F and G are consistent with as much as 45 m maximum post-$Q2_b$ slip on Helendale fault. (See footnote 1 for additional figures depicting restorations of offsets and photographs of slip-rate sites.) UTM—Universal Transverse Mercator.

2003). Most ductile deformation likely occurs in the dislocation (power law) creep regime, where strain rate is set by the rate of recovery processes that counteract work hardening (Tsenn and Carter, 1987; Hirth and Tullis, 1992). Thus in the absence of other mechanisms, power-law creep is unlikely to lead to the observed variation of loading rate.

We hypothesize that one or more feedback mechanisms link clusters of large earthquakes to transient weakening of shear zones. In the semi-brittle regime, coseismic fracture may periodically introduce fluids that enhance power-law creep (Hirth and Tullis, 1992) and lower frictional strength (Chester, 1995). High postseismic stresses may also induce grain-size reduction, enhancing diffusion creep and grain-boundary sliding (e.g., Montési and Hirth, 2003). These mechanisms could promote positive feedback between earthquakes and weakening of shear zones consistent with the prolonged (~1 k.y.) periods of clustered earthquake activity inferred from paleoseismic records (Rockwell et al., 2000; Dolan et al., 2007). Strengthening of ductile shear zones could result as fluids are consumed in metamorphic reactions and grain size equilibrates to ambient stress. Strain hardening may also arise from pinning of brittle fault tips against a kinematically incompatible intersecting fault, such as occurs where dextral faults of the ECSZ meet the sinistral Garlock fault (Fig. 1). Such a mechanism could drive oscillation of loading between these conjugate systems, as proposed by Peltzer et al. (2001).

CONCLUSION

New fault slip-rate data from the ECSZ establish that an ongoing cluster of earthquake activity here is accompanied by an ~2× average tectonic loading rate. This elevated loading directly increases seismic hazard (Dieterich, 1994). We attribute elevated loading to transient strain weakening of ductile shear zones, and hypothesize that major earthquakes promote this strain weakening and lead to positive feedback that gives rise to earthquake clustering. Recognition of an elevated strain accumulation rate with attendant changes in major earthquake activity has far-reaching implications for time-dependent seismic hazard. For areas where earthquake clusters have been recognized, such as the Los Angeles region (Dolan et al., 2007), an active (inactive) strain accumulation mode could substantially increase (decrease) earthquake risk.

TABLE 1. FAULT OFFSETS, AGES, AND SLIP RATES IN THE EASTERN CALIFORNIA SHEAR ZONE

Fault	Offset (m)	Age (ka)	Slip rate (mm/yr)
Helendale*	≤45	56 ± 21	≤0.8 ± 0.3
Lenwood†	29 ± 5	37 ± 7	0.8 ± 0.2
Camp Rock*	≤70	≥50 ± 20	≤1.4 ± 0.6
Calico	100 ± 10	57 ± 9	1.8 ± 0.3
Pisgah-Bullion	725 ± 85	752 ± 110	1.0 ± 0.2
Ludlow	19 ± 4	≥50 ± 20	≤0.4 ± 0.2

Note: Errors added in quadrature. Sum of slip rates is ≤6.2 ± 1.9 mm/yr. Sum error includes ^{10}Be production rate uncertainty.

*Maximum offset used to calculate maximum rate.

†Using minimum 19 m offset lowers minimum Lenwood fault slip rate to 0.5 mm/yr.

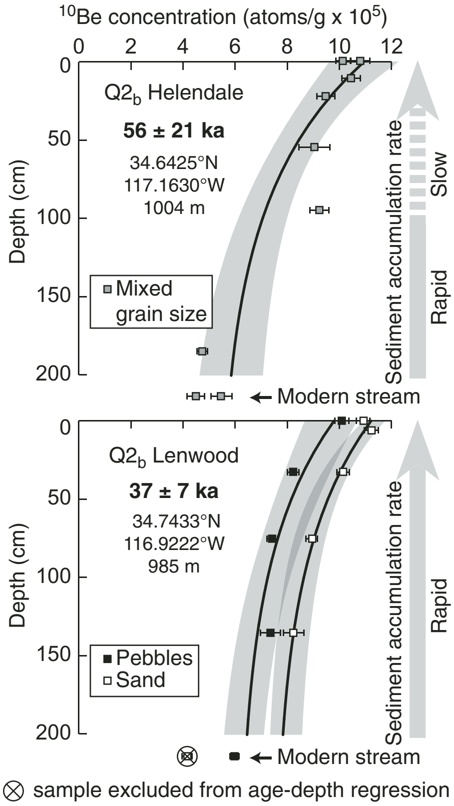

Figure 3. Depth profiles of ^{10}Be concentration from Q2$_b$ fans adjacent to Helendale and Lenwood faults with modeled surface ages (for ^{10}Be concentration data, see Data Repository [see footnote 1]). We use a value of 2.0 g/cm^2 for sediment bulk density, typical for unconsolidated, poorly sorted alluvium. Gray bands depict 95% standard error of mean concentration as exponential function of depth. For the Lenwood fault, we found that inheritance was less for pebble-sized samples than for sand. These independent curves yield identical mean ages of 37 ka; 95% confidence of ±7 ka was determined by normalizing to common inheritance. For Helendale fault, we analyzed bulk samples with sand- through small-pebble-sized grains and did not resolve grain-size dependent inheritance. Slowing of sediment accumulation rate in upper part of Helendale profile, evidenced in the field by anomalously thick argillic soil, could have resulted in excess inherited ^{10}Be acquired during sediment burial. Mean ages modeled with 0.02 ± 0.01 mm/yr sediment accumulation in upper 50–100 cm ranged from 55 ka to 59 ka, indistinguishable from mean age assuming uniform sediment accumulation rate. Modern stream samples, shown below each graph, are overall consistent with shielded ^{10}Be concentrations at depth. We attribute low ^{10}Be in modern stream sand at Lenwood fault site to Holocene eolian input.

ACKNOWLEDGMENTS

This work is based upon work supported by the National Science Foundation under grant number EAR-0337263, with additional support from grants EAR-0516760 and EAR-0337667. We thank J. Dolan and T. Dixon for their helpful reviews, and the National Center for Airborne Laser Mapping for providing research-grade topographic surveys.

REFERENCES CITED

Anderson, R.S., Repka, J.L., and Dick, G.S., 1996, Explicit treatment of inheritance in dating depositional surfaces using in situ ^{10}Be and ^{26}Al: Geology, v. 24, p. 47–51, doi: 10.1130/0091–7613(1996)024<0047:ETOIID>2.3.CO;2.

Bennett, R.A., Wernicke, B.P., Niemi, N.A., Friedrich, A.M., and Davis, J.L., 2003, Contemporary strain rates in the northern Basin and Range province from GPS data: Tectonics, v. 22, doi: 10.1029/2001TC001355.

Bull, W.B., 1991, Geomorphic responses to climatic change: New York, Oxford University Press, 326 p.

Chester, F., 1995, A rheologic model for wet crust applied to faults: Journal of Geophysical Research, v. 100, p. 13,033–13,044, doi: 10.1029/95JB00313.

Dawson, T., McGill, S.F., and Rockwell, T.K., 2003, Irregular recurrence of paleoearthquakes along the central Garlock fault near El Paso Peaks, California: Journal of Geophysical Research, v. 108, doi: 10.1029/2001JB001744.

Dibblee, T.W., 1961, Evidence of strike-slip movement on northwest-trending faults in Mojave Desert, California, *in* Short papers in the geologic and hydrologic sciences: Geological Survey research 1961: U.S. Geological Survey Professional Paper 424-B, p. 197–198.

Dieterich, J.H., 1994, A constitutive law for rate of earthquake production and its application to earthquake clustering: Journal of Geophysical Research, v. 99, p. 2601–2618, doi: 10.1029/93JB02581.

Dixon, T.H., Norabuena, E., and Hotaling, L., 2003, Paleoseismology and Global Positioning System: Earthquake-cycle effects and geodetic versus geologic fault slip rates in the Eastern California shear zone: Geology, v. 31, p. 55–58, doi: 10.1130/0091–7613(2003)031<0055:PAGPSE>2.0.CO;2.

Dolan, J.F., Bowman, D.D., and Sammis, C.G., 2007, Long-range and long-term fault interactions in southern California: Geology, v. 35, p. 855–858, doi: 10.1130/G23789A.1.

Freed, A.M., Bürgmann, R., and Herring, T., 2007, Far-reaching transient motions after Mojave earthquakes require broad mantle flow beneath a strong crust: Geophysical Research Letters, v. 34, doi: 10.1029/2007GL030959.

Hart, E.W., Bryant, W.A., Kahle, J.E., Manson, M.W., and Bortugno, W.J., 1988, Summary report: Fault Evaluation Program, 1986–1987, Mojave Desert region and other areas: California Department of Conservation, Division of Mines and Geology Open-File Report 88–1, 40 p.

Hirth, G., and Tullis, J., 1992, Dislocation creep regimes in quartz aggregates: Journal of Structural Geology, v. 14, p. 145–159, doi: 10.1016/0191–8141(92)90053-Y.

Kagan, Y.Y., and Jackson, D.D., 1991, Long-term earthquake clustering: Geophysical Journal International, v. 104, p. 117–133, doi: 10.1111/j.1365–246X.1991.tb02498.x.

Marco, S., Stein, M., Agnon, A., and Ron, H., 1996, Long-term earthquake clustering: A 50,000-year paleoseismic record in the Dead Sea graben: Journal of Geophysical Research, v. 101, p. 6179–6192, doi: 10.1029/95JB01587.

Meade, B.J., and Hager, B.H., 2005, Block models of crustal motions in southern California constrained by GPS measurements: Journal of Geophysical Research, v. 110, doi:10.1029/2004JB003209.

Montési, L.G.J., and Hirth, G., 2003, Grain size evolution and the rheology of ductile shear zones: From laboratory experiments to postseismic creep: Earth and Planetary Science Letters, v. 211, p. 97–110, doi: 10.1016/S0012–821X(03)00196–1.

Oskin, M.E., Perg, L.A., Blumentritt, D., Mukhopadhyay, S., and Iriondo, A., 2007, Slip rate of the Calico fault: Implications for geologic versus geodetic discrepancy in the Eastern California shear zone: Journal of Geophysical Research, v. 112, doi: 10.1029/2006JB004451.

Peltzer, G., Crampé, F., Hensley, S., and Rosen, P., 2001, Transient strain accumulation and fault interaction in the Eastern California shear zone: Geology, v. 29, p. 975–978, doi: 10.1130/0091–7613(2001)029<0975:TSAAFI>2.0.CO;2.

Pollitz, F.F., Vergnolle, M., and Calais, E., 2003, Fault interaction and stress triggering of twentieth century earthquakes in Mongolia: Journal of Geophysical Research, v. 108, doi: 10.1029/2002JB002375.

Rockwell, T.K., Lindvall, S., Herzberg, M., Murbach, D., Dawson, T., and Berger, G., 2000, Paleoseismology of the Johnson Valley, Kickapoo, and Homestead Valley faults: Clustering of earthquakes in the Eastern California shear zone: Seismological Society of America Bulletin, v. 90, p. 1200–1236, doi: 10.1785/0119990023.

Rymer, M.J., Seitz, G.G., Weaver, K.D., Orgil, A., Faneros, G., Hamilton, J.C., and Goetz, C., 2002, Geologic and paleoseismic study of the Lavic Lake fault at Lavic Lake Playa, Mojave Desert, southern California: Seismological Society of America Bulletin, v. 92, p. 1577–1591, doi: 10.1785/0120000936.

Sauber, J., Thatcher, W., Solomon, S.C., and Lisowski, M., 1994, Geodetic slip rate for the eastern California shear zone and the recurrence time of Mojave Desert earthquakes: Nature, v. 367, p. 264–266, doi: 10.1038/367264a0.

Savage, J.C., and Lisowski, M., 1998, Viscoelastic coupling model of the San Andreas fault along the big bend, southern California: Journal of Geophysical Research, v. 103, p. 7281–7292, doi: 10.1029/98JB00148.

Stone, J.O., 2000, Air pressure and cosmogenic isotope production: Journal of Geophysical Research, v. 105, p. 23,753–23,759, doi: 10.1029/2000JB900181.

Trepmann, C.A., and Stöckhert, B., 2003, Quartz microstructures developed during non-steady state plastic flow at rapidly decaying stress and strain rate: Journal of Structural Geology, v. 25, p. 2035–2051, doi: 10.1016/S0191–8141(03)00073–7.

Tsenn, M.C., and Carter, N.L., 1987, Upper limits of power law creep of rocks: Tectonophysics, v. 136, p. 1–26, doi: 10.1016/0040–1951(87)90332–5.

Wells, R., and Hillhouse, J., 1989, Paleomagnetism and tectonic rotation of the lower Miocene Peach Spring Tuff: Colorado Plateau, Arizona, to Barstow, California: Geological Society of America Bulletin, v. 101, p. 846–863, doi: 10.1130/0016–7606(1989)101<0846:PATROT>2.3.CO;2.

Manuscript received 25 January 2008
Revised manuscript received 27 February 2008
Manuscript accepted 3 March 2008

Printed in USA